湖南科技大學
Hunan University of Science and Technology

各向同性热密物质中的QCD轴子性质研究

Zhen-Yan Lu (陆振烟)

Email: luzhenyan@hnust.edu.cn

湖南科技大学物理系

第九届手征有效场论研讨会，湖南长沙

2024年10月18日—10月22日

Outline

湖南科技大學
Hunan University of Science and Technology

☼ Introduction

☼ Axion properties at nonzero temperature and baryon density

☼ Summary

Outline

湖南科技大學
Hunan University of Science and Technology

- Introduction
- Axion properties at nonzero temperature and baryon density
- Summary

QCD Lagrangian

The massless QCD Lagrangian

$$\mathcal{L}^0_{QCD} = \sum_{f=1}^{N} \bar{q}_f i\gamma^\mu D_\mu q_f - \frac{1}{4} G^c_{\mu\nu} G^{c,\mu\nu}$$

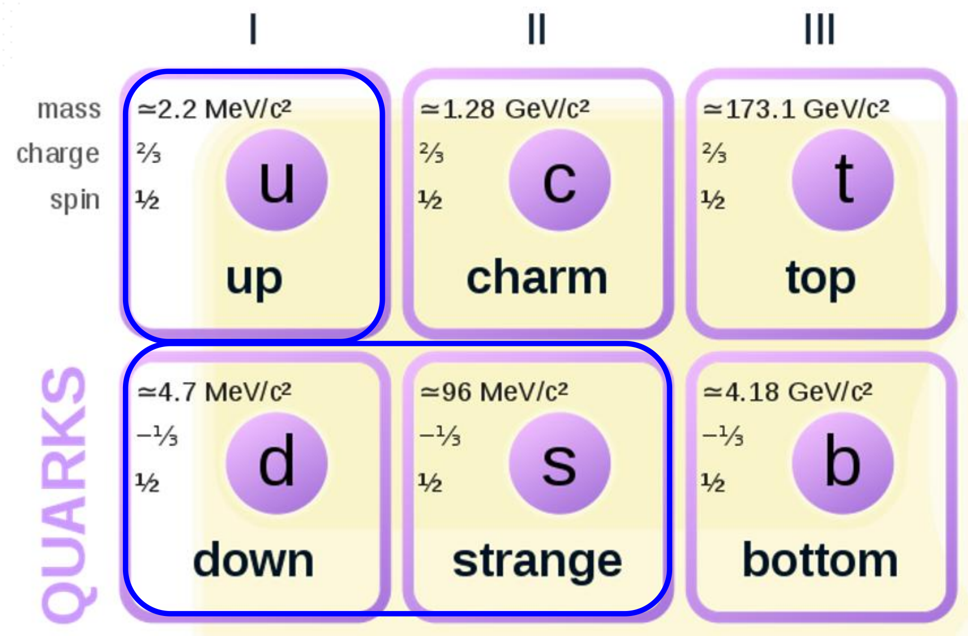

The gluon field tensor

$$G^c_{\mu\nu} = \partial_\mu A^c_\nu - \partial_\nu A^c_\mu - g_s f_{abc} A^b_\mu A^c_\nu$$

Gluon self-interacting

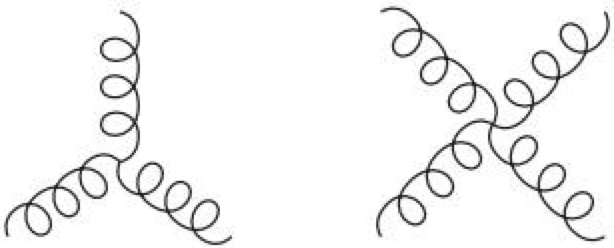

High energies

- asymptotic freedom, perturbative

Low energies

- color confinement, nonperturbative

Energy density: At finite isospin chemical potential

湖南科技大學
Hunan University of Science and Technology

QCD: the theory of strong interaction (chiral symmetry)

- In the non-perturbative regime, one must resort to
  - ☐ Perturbative QCD (pQCD) → High densities ✓
  - ☐ Chiral Perturbation theory (CHPT, χ PT) → Low densities ✓
  - ☐ First principle calculation (Lattice QCD)
  - ☐ Effective models

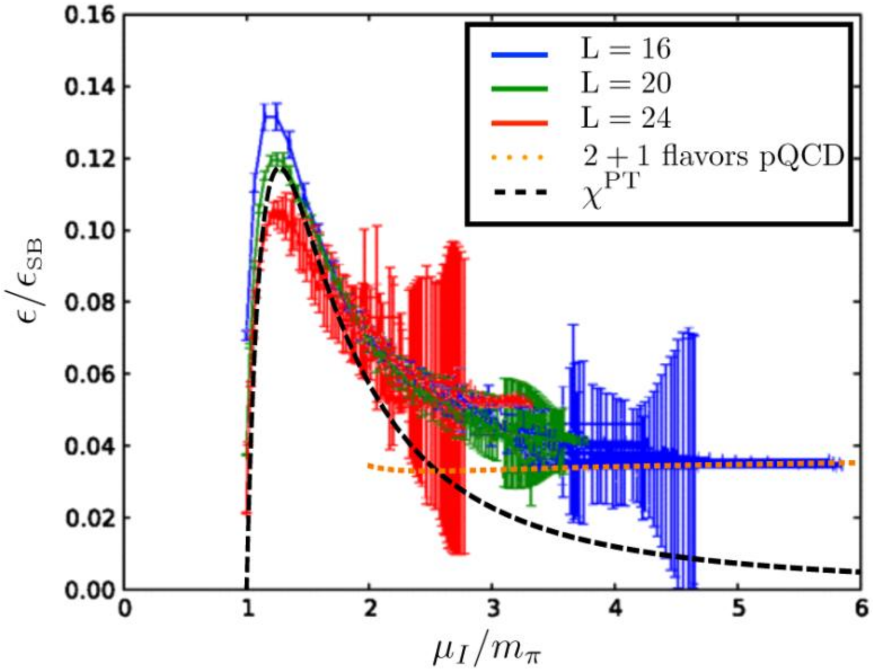

Carignano, A. Mammarella, and M. Mannarelli, Phys. Rev. D 93, 051503 (2016)

Peak structure: At finite isospin chemical potential

The conformal relation $E = 3P$ is satisfied at

$$\bar{\mu}_I \simeq 1.754 m_\pi \quad \text{NJL}$$

$$\bar{\mu}_I = \sqrt{3} m_\pi \quad \text{CHPT}$$

(the NJL results)
In good agreement with the results obtained in CHPT and lattice simulation

Comparison: **The peak position** of the energy density over the Stefan-Boltzmann limit

$$\mu_I^{\text{peak}} \simeq \begin{cases} 1.274 m_\pi, & \text{NJL} \\ 1.276 m_\pi, & \text{CHPT} \\ \{1.20, 1.25, 1.275\} m_\pi, & \text{Lattice data} \end{cases}$$

n_I and pressure: At finite isospin chemical potential

Isospin number density: $n_I = -\dfrac{\partial\Omega}{\partial\mu_I}$

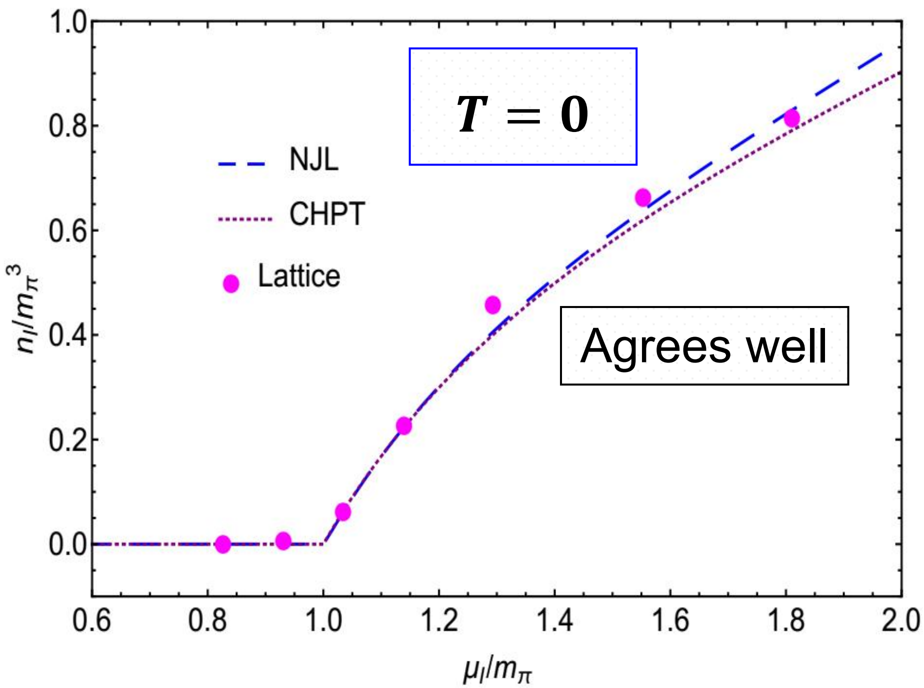

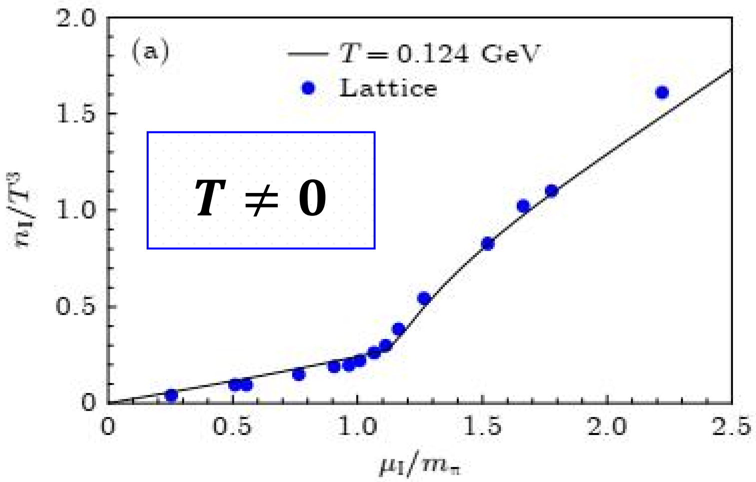

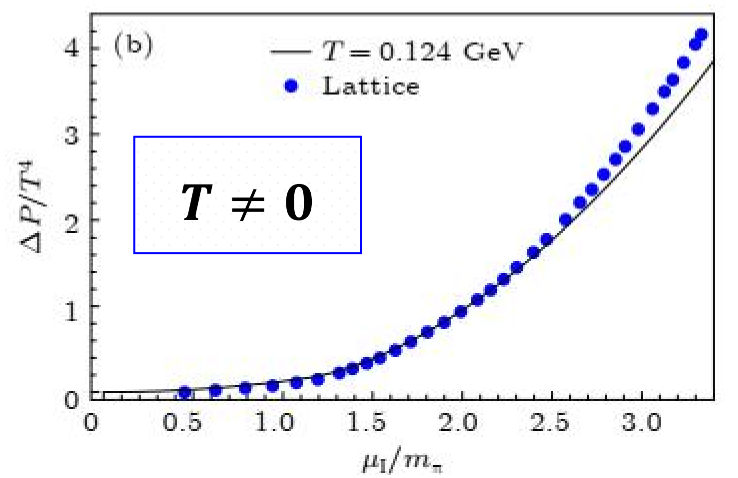

ZYL, C.-J. Xia, and M. Ruggieri, Eur. Phys. J. C 80, 46 (2020)

卢琪, 陈伟杰, 陆振烟等. 物理学报 70, 145101 (2021)

QCD at finite T and μ_B

湖南科技大學
Hunan University of Science and Technology

QCD at finite temperature and baryon chemical potential

- Early universe
- Heavy ion collision experiments
- Compact stars (e.g. neutron stars, quark stars)

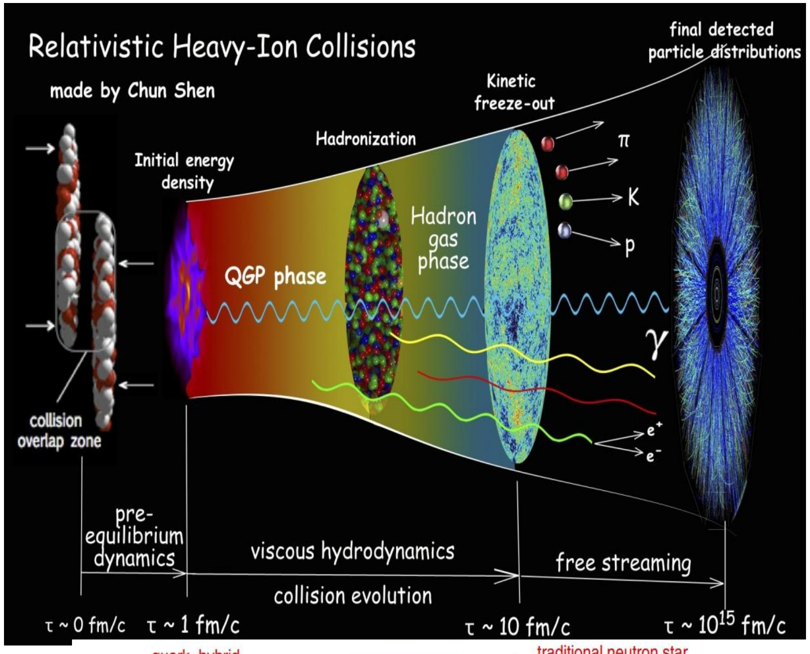

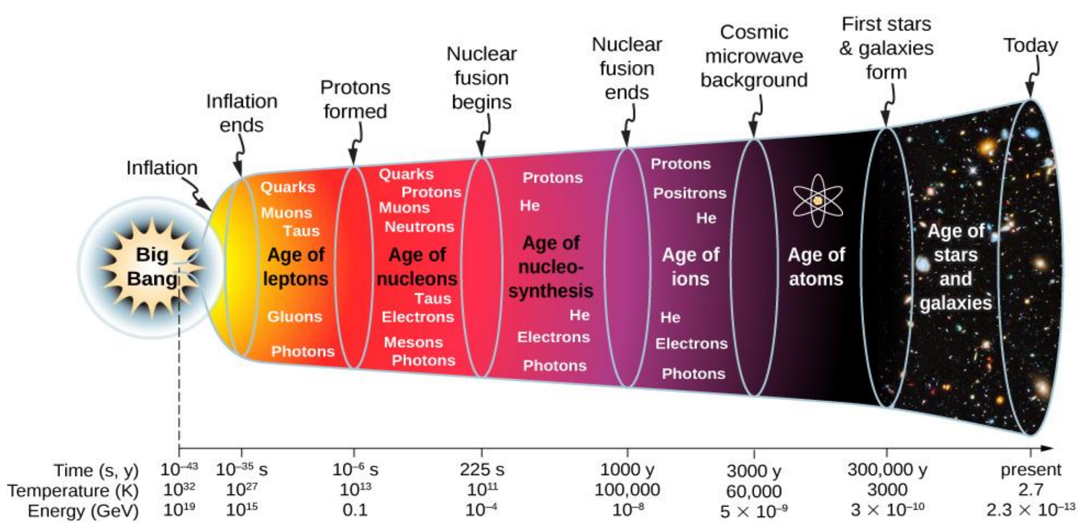

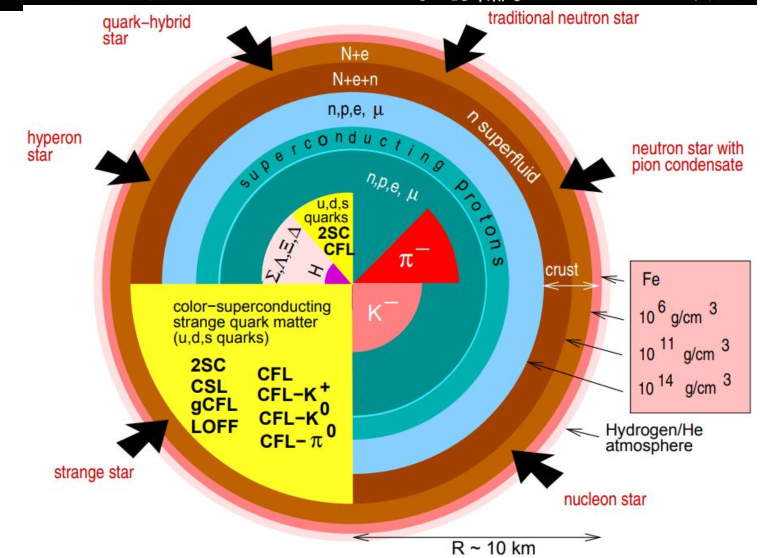

Outline

湖南科技大學
Hunan University of Science and Technology

- ☼ Introduction
- ☼ Axion properties at nonzero temperature and baryon density
- ☼ Summary

NJL model calculation

Two-flavor NJL model Lagrangian

$$\mathcal{L} = \bar{q}(i\gamma^\mu \partial_\mu - m)q + \mathcal{L}_{\bar{q}q} + \mathcal{L}_{\rm det}$$

with $\mathcal{L}_{\bar{q}q} = G_1[(\bar{q}\tau_a q)^2 + (\bar{q}\tau_a i\gamma_5 q)^2]$ *and* $\mathcal{L}_{\rm det} = 8G_2\left[e^{i\frac{a}{f_a}}\det(q_R q_L) + e^{-i\frac{a}{f_a}}\det(q_L q_R)\right]$

The thermodynamic potential in the mean field approximation

$$\Omega(\alpha_0, \beta_0) = \Omega_q + G_2(\eta^2 - \sigma^2)\cos\frac{a}{f_a} - G_1(\eta^2 + \sigma^2) + 2G_2\sigma\eta\sin\frac{a}{f_a}$$

ZYL and M. Ruggieri,
Phys. Rev. D 100, 014013 (2019)

where the quark contribution reads

$$\Omega_q = -8N_c\int\frac{\mathrm{d}^3p}{(2\pi)^3}\left[\frac{E_p}{2} + T\log\left(1 + e^{-E_p/T}\right)\right]$$

$$\begin{cases} E_p = \sqrt{p^2 + M^2}, \quad M = \sqrt{(m + \alpha_0)^2 + \beta_0^2} \\ \alpha_0 = -2\left(G_1 + G_2\cos\frac{a}{f_a}\right)\sigma + 2G_2\eta\sin\frac{a}{f_a} \\ \beta_0 = -2\left(G_1 - G_2\cos\frac{a}{f_a}\right)\eta + 2G_2\sigma\sin\frac{a}{f_a} \end{cases}$$

Effective potential for axion

湖南科技大學
Hunan University of Science and Technology

The effective potential depends on the axion field explicitly and implicitly

$$\frac{\mathrm{d}\mathcal{V}}{\mathrm{d}a} = \frac{\partial \mathcal{V}}{\partial a} + \frac{\partial \mathcal{V}}{\partial \sigma}\frac{\partial \sigma}{\partial a} + \frac{\partial \mathcal{V}}{\partial \eta}\frac{\partial \eta}{\partial a}$$

The gap equations

$$\frac{\partial \Omega}{\partial \sigma}\Big|_{\sigma=\bar{\sigma}} = 0 \qquad \frac{\partial \Omega}{\partial \eta}\Big|_{\eta=\bar{\eta}} = 0$$

The effective potential for the axion

$$\mathcal{V}(a) = \Omega(\sigma = \bar{\sigma}, \eta = \bar{\eta}|a)$$

The axion mass

$$m_a^2 = \frac{\mathrm{d}^2\mathcal{V}(a)}{\mathrm{d}a^2}\Big|_{a=0} = f_a^2 \chi_t$$

The axion self-coupling constant

$$\lambda_a = \frac{\mathrm{d}^4\mathcal{V}(a)}{\mathrm{d}a^4}\Big|_{a=0}$$

Topological susceptibility

湖南科技大學
Hunan University of Science and Technology

The topological susceptibility from chiral perturbation theory up to next-to-leading order with non-degenerate quark masses

$$\chi_{\rm top}^{1/4} = \sqrt{m_a f_a} = 75.5(5)\,\mathrm{MeV}$$

The topological susceptibility in the isospin symmetric case

Chiral perturbation theory $$\chi_t^{1/4} = 77.8(4)\ \mathrm{MeV}$$

G. G. di Cortona, E. Hardy, J. P. Vega, and G. Villadoro, J. High Energy Phys. 2016, 34 (2016)

NJL model $$\chi_t^{1/4} = 79.87\ \mathrm{MeV}$$

ZYL and M. Ruggieri, Phys. Rev. D 100, 014013 (2019)

Lattice simulation $$\chi_t^{1/4} = 78.1(2)\ \mathrm{MeV}$$

S. Borsanyi, Z. Fodor, J. Guenther, K.-H. Kampert, S. D. Katz, and et al., Nature 539, 69 (2016)

Axion properties: At zero temperature

湖南科技大學
Hunan University of Science and Technology

At zero temperature

Chiral perturbation theory

$$\begin{cases} m_a = 6.06(5) \times \frac{10^3}{f_a} \text{ MeV}^2 \\ \lambda_a = -\left(\frac{55.64 \text{ MeV}}{f_a}\right)^4 \end{cases}$$

G. G. di Cortona, E. Hardy, J. P. Vega, and G. Villadoro, J. High Energy Phys. 2016, 34 (2016)

NJL model

$$\begin{cases} m_a = 6.38 \times \frac{10^3}{f_a} \text{ MeV}^2 \\ \lambda_a = -\left(\frac{55.79(92) \text{ MeV}}{f_a}\right)^4 \end{cases}$$

ZYL and M. Ruggieri, Phys. Rev. D 100, 014013 (2019)

Chiral condensate and self-coupling constant

湖南科技大學
Hunan University of Science and Technology

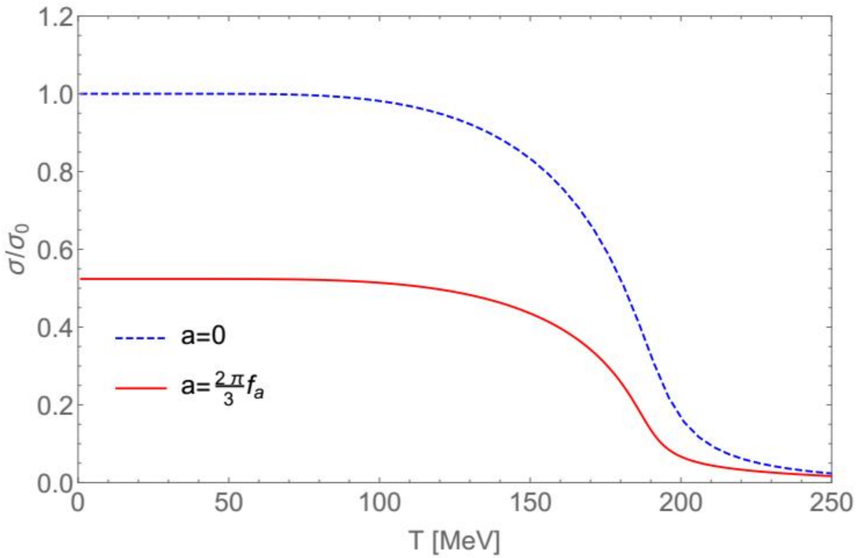

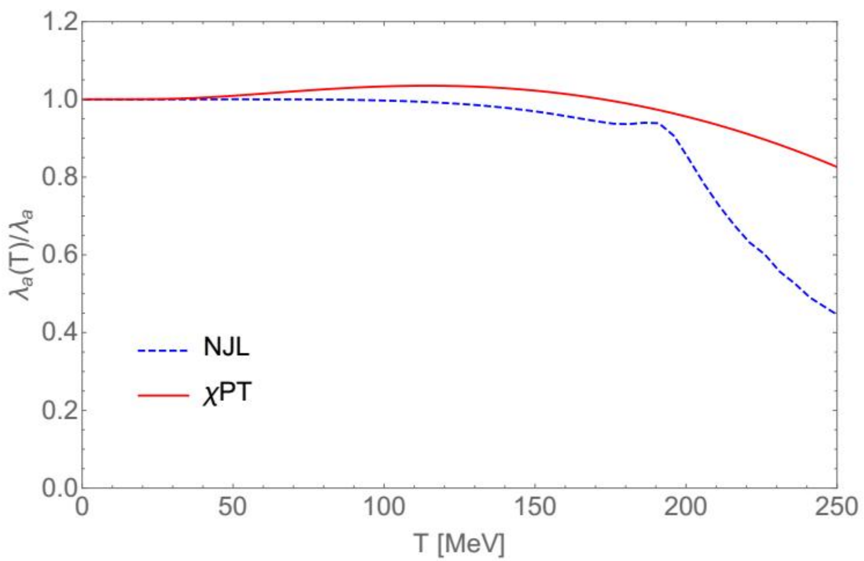

- The chiral condensate, scaled by its zero temperature value, as a function of the temperature.

ZYL and M. Ruggieri, Phys. Rev. D 100, 014013 (2019)

NJL model at finite baryon chemical potential

湖南科技大學
Hunan University of Science and Technology

The Lagrangian density of the two-flavor NJL model is given by

$$\mathcal{L} = \bar{q}\left(i\gamma^{\mu}\partial_{\mu} + \mu\gamma_0 - m_0\right)q + \mathcal{L}_{\text{int}}$$

with

$$\begin{aligned}\mathcal{L}_{\text{int}} =& G_1\left[\left(\bar{q}\tau_a q\right)\left(\bar{q}\tau_a q\right) + \left(\bar{q}i\tau_a\gamma_5 q\right)\left(\bar{q}i\tau_a\gamma_5 q\right)\right] \\ &+ 8G_2\left[e^{i\theta}\det\left(\bar{q}_R q_L\right) + e^{-i\theta}\det\left(\bar{q}_L q_R\right)\right]\end{aligned}$$

Mean field approximation

$$\begin{aligned}(\bar{q}q)^2 &\approx 2(\bar{q}q)\langle\bar{q}q\rangle - \langle\bar{q}q\rangle^2, \\ (\bar{q}i\tau_a\gamma_5 q)^2 &\approx 2(\bar{q}i\tau_a\gamma_5 q)\langle\bar{q}i\tau_a\gamma_5 q\rangle - \langle\bar{q}i\tau_a\gamma_5 q\rangle^2,\end{aligned}$$

The thermodynamic potential of the system $\Omega = \Omega_{\text{mf}} + \Omega_q$

with

$$\begin{aligned}\Omega_{\text{mf}} =& -G_2\left(\eta^2 - \sigma^2\right)\cos\theta + G_1\left(\eta^2 + \sigma^2\right) \\ &- 2G_2\sigma\eta\sin\theta,\end{aligned}$$

and

$$\begin{aligned}\Omega_q =& -2N_c T\sum_{f=u,d}\int\frac{d^3p}{(2\pi)^3}\left\{\frac{E_p}{T}\right. \\ &\left.+\ln\left[1 + e^{-(E_p-\mu_f)/T}\right] + \ln\left[1 + e^{-(E_p+\mu_f)/T}\right]\right\}\end{aligned}$$

Chiral condensate

H.-F. Gong, Q. Lu, ZYL, L.-M. Liu, X. Chen, and S.-P. Wang, (2024), arXiv:2404.15136 [hep-ph].

Order parameter of the chiral symmetry: chiral condensate σ

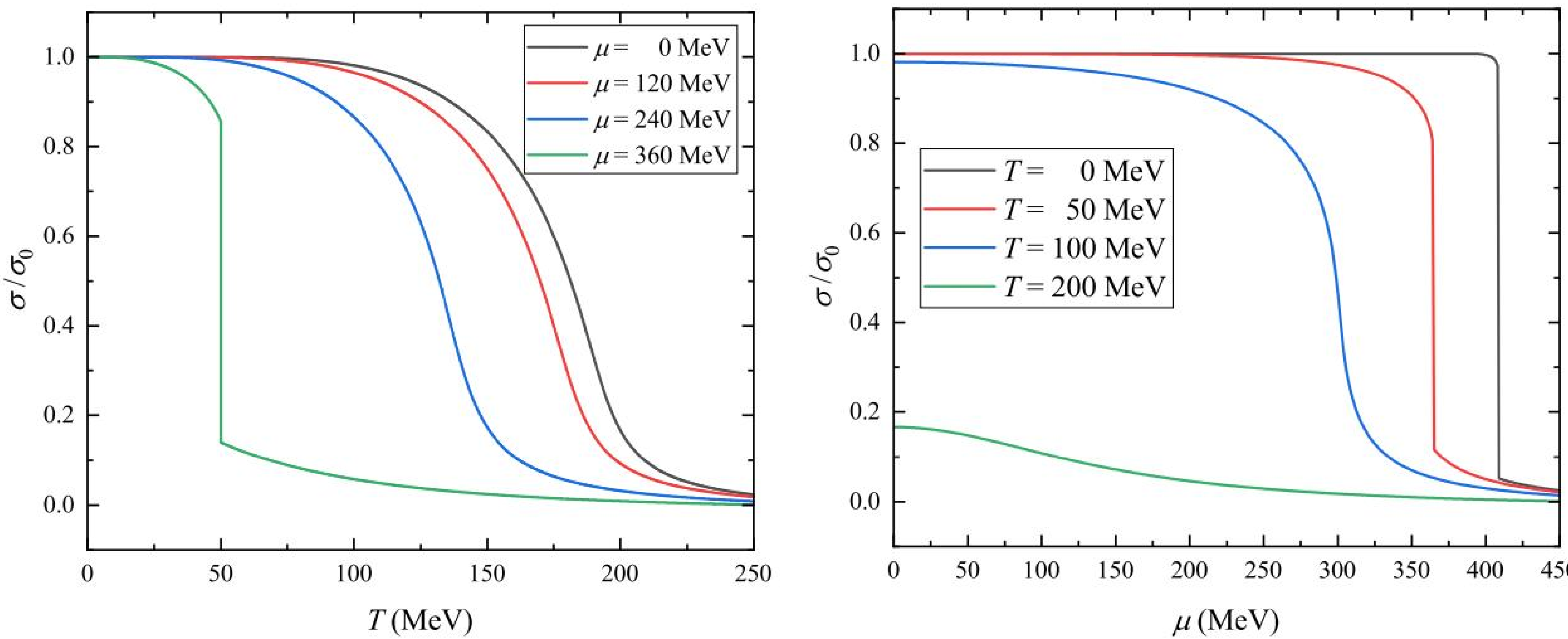

- Variation of the chiral condensate, scaled by its value in the vacuum, with respect to the temperature at different chemical potentials (left panel) and to the chemical potential at different temperatures (right panel), respectively.

Topological susceptibility

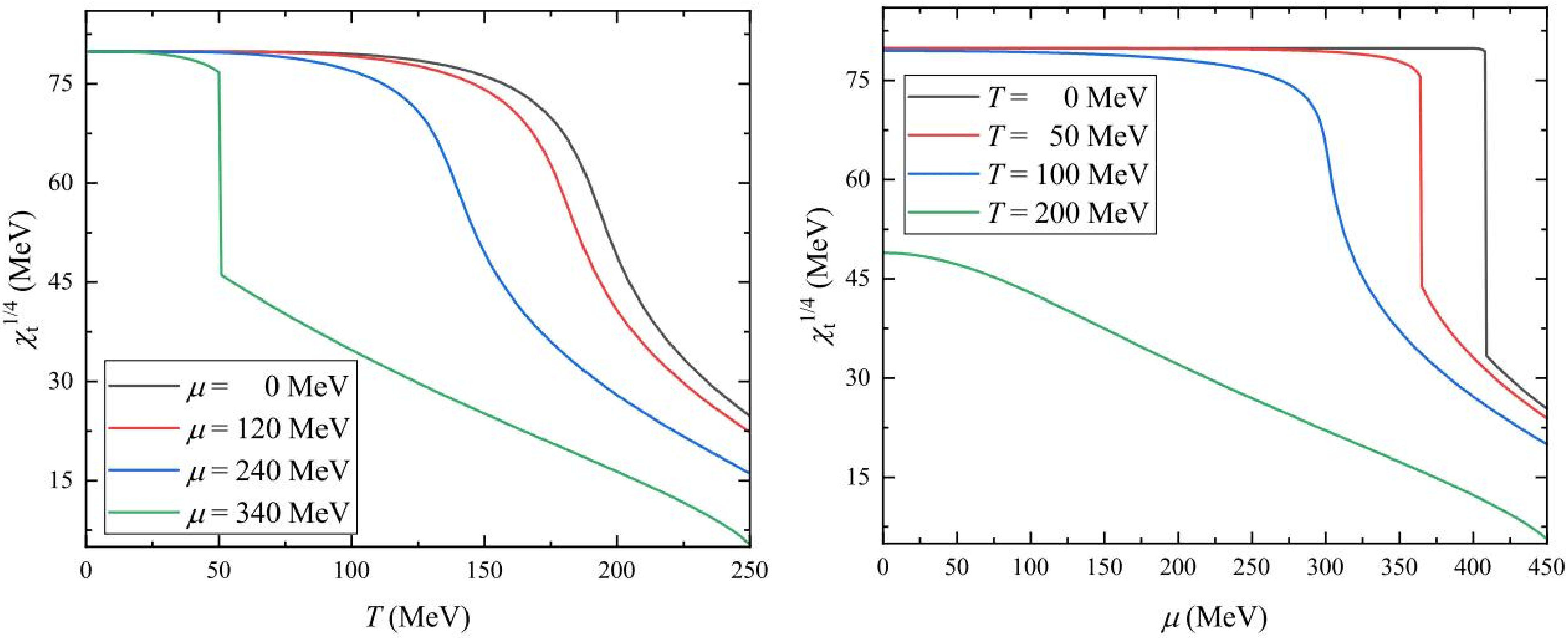

- Variation of the topological susceptibility, scaled by its value in the vacuum, with respect to the temperature at different chemical potentials (left panel) and to the chemical potential at different temperatures (right panel), respectively.

Normalized fourth cumulant

湖南科技大學
Hunan University of Science and Technology

$$b_2 = \frac{1}{12\chi_t} \frac{d^4 \mathcal{V}(\theta, T, \mu)}{d\theta^4}\bigg|_{\theta=0}$$

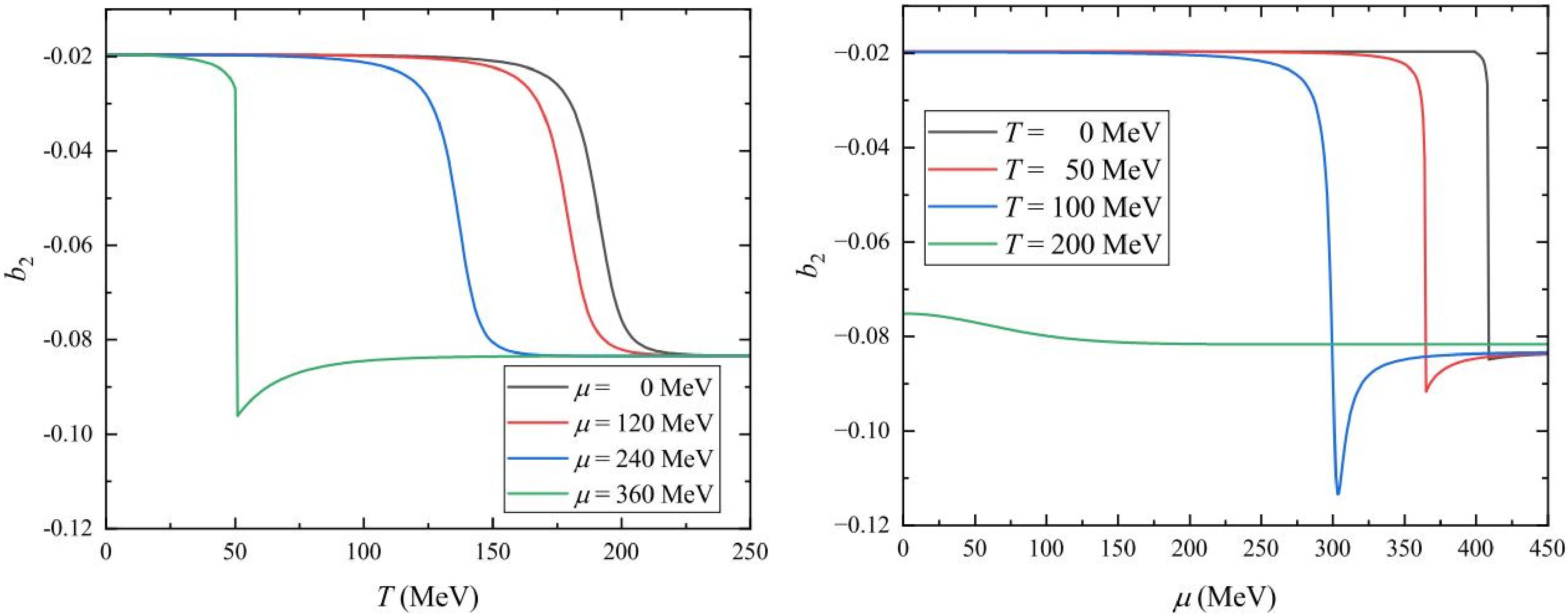

- Variation of the normalized fourth cumulant, scaled by its value in the vacuum, with respect to the temperature at different chemical potentials (left panel) and to the chemical potential at different temperatures (right panel), respectively.

Axion mass

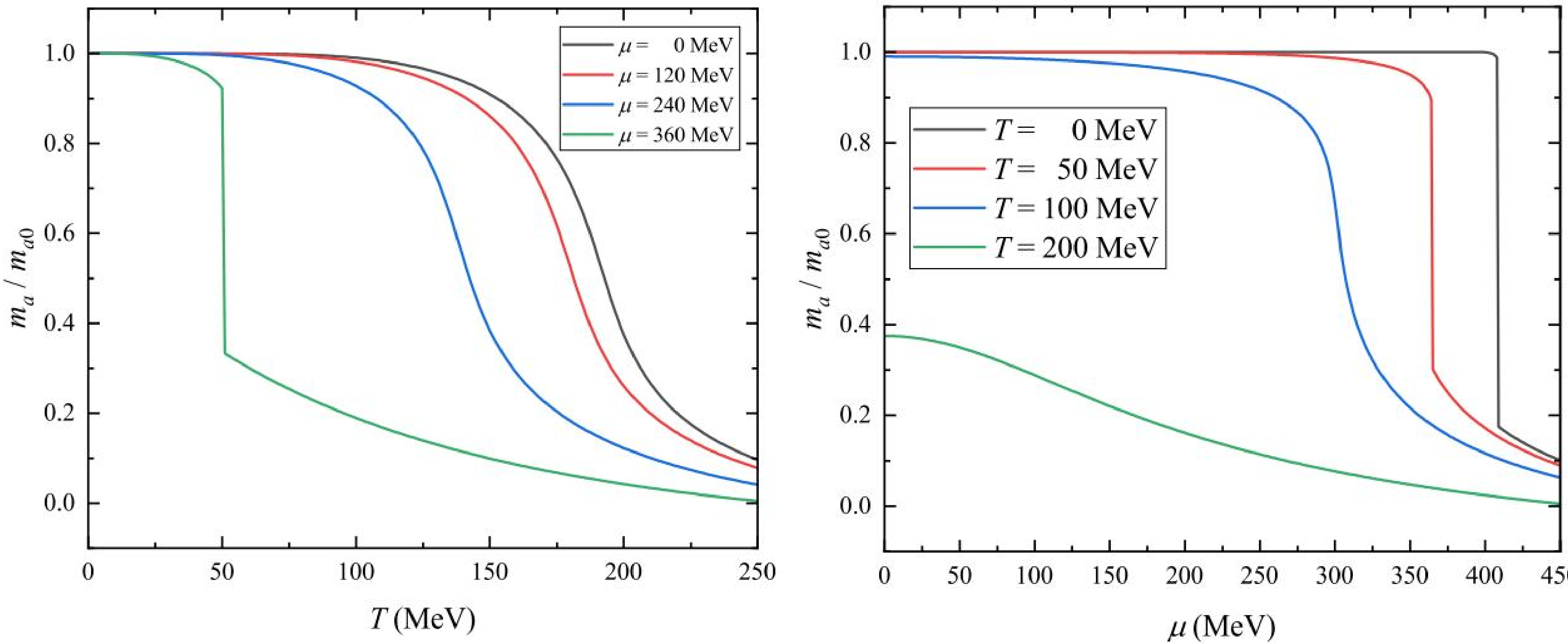

- Variation of the axion mass, scaled by its value in the vacuum, with respect to the temperature at different chemical potentials (left panel) and to the chemical potential at different temperatures (right panel), respectively.

Axion self-coupling constant

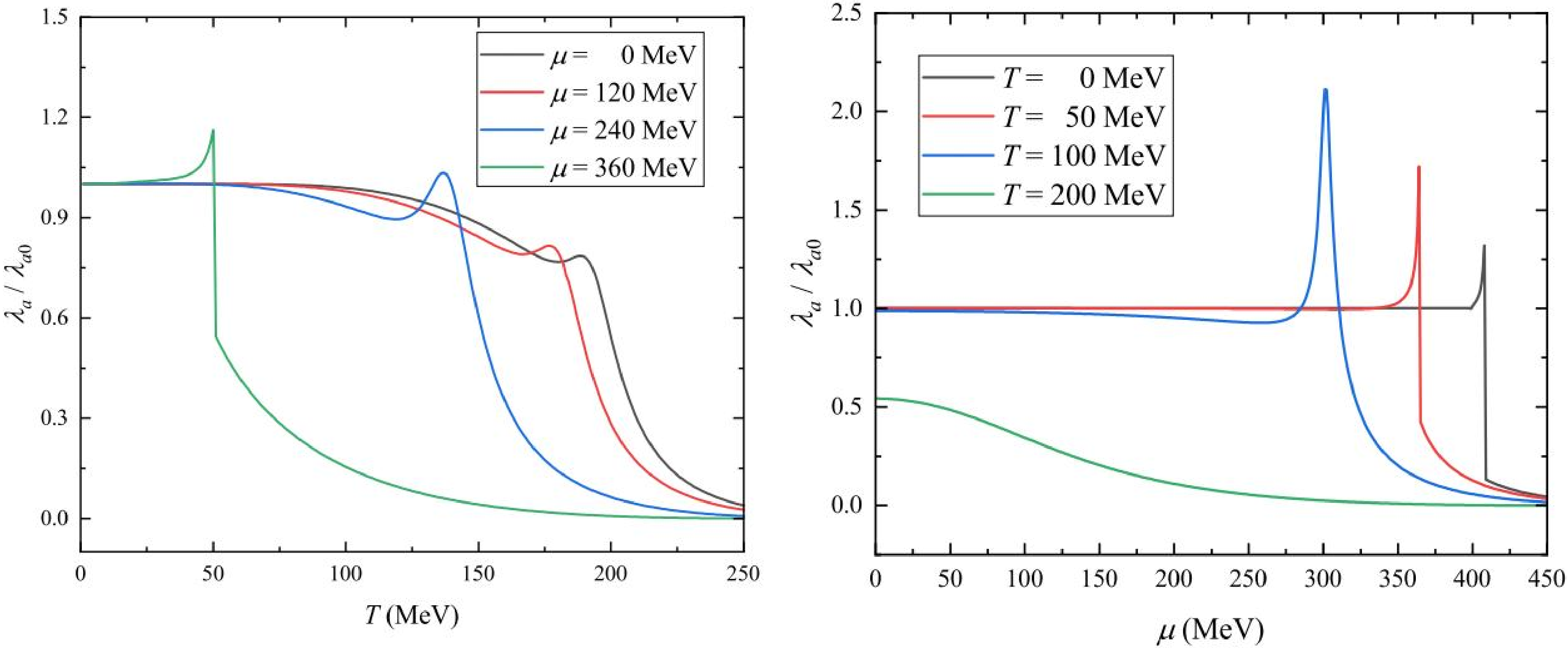

- Variation of the axion self-coupling constant, scaled by its value in the vacuum, with respect to the temperature at different chemical potentials (left panel) and to the chemical potential at different temperatures (right panel), respectively.

Outline

湖南科技大學
Hunan University of Science and Technology

- Introduction
- Axion properties at nonzero temperature and baryon density
- Summary

Summary

● The **topological susceptibility and the axion mass** follow the response of the chiral condensate to temperature and chemical potential, showing that both quantities **decrease monotonically with the increment of temperature and/or chemical potential.**

● The **axion self-coupling constant exhibits a sharp peak around the critical point**, which can even be more than twice its vacuum value.

● The **chiral phase transition** significantly **reduces the axion mass** while considerably **enhancing the self-coupling constant**.

Thank You！

湖南科技大學
Hunan University of Science and Technology